PERGAMON

International Journal of Multiphase Flow 28 (2002) 865–880

International Journal of Multiphase Flow

www.elsevier.com/locate/ijmulflow

Non-intrusive determination of bubble and slug length scales in fluidized beds by decomposition of the power spectral density of pressure time series

J. van der Schaaf [a,b,*], J.C. Schouten [b], F. Johnsson [c], C.M. van den Bleek [a]

[a] *Chemical Reactor Engineering Section, Department of Chemical Process Technology, J.M. Burgers Centre for Fluid Mechanics, Delft University of Technology, Julianalaan 136, 2628 BL Delft, Netherlands*

[b] *Laboratory of Chemical Reactor Engineering, Eindhoven University of Technology, P.O. Box 513, 5600 MB Eindhoven, Netherlands*

[c] *Department of Energy Conversion, Chalmers University of Technology, S-412 96 Göteborg, Sweden*

Received 30 November 1999; received in revised form 29 November 2001

Abstract

In this paper we show that spectral analysis of non-intrusive time dependent pressure measurements in bubbling and circulating gas–solid fluidized beds permits to obtain the first estimates of bubble, gas slug, and solids cluster length scales from pressure fluctuation data. These length scales are calculated from the incoherent cross power spectra of pressure signals measured in the bubbling or circulating bed and in the plenum. Remarkable quantitative agreement with bubble diameter data is found, and equally remarkable agreement is obtained with independent estimates of gas slug lengths by others in circulating fluidized beds. These results demonstrate the possibility of greatly expanding the information that can be obtained non-intrusively from gas–solid fluidized beds. © 2002 Published by Elsevier Science Ltd.

Keywords: Fluidization; Bubble size; Slug size; Pressure; Power spectral density; Coherence

1. Introduction

A gas–solid fluidized bed is a commonly encountered reactor type in chemical industries for, e.g., efficiently contacting gaseous reactants with catalyst particles. Because the performance of a fluidized bed is highly dependent on the hydrodynamic state of fluidization, fluidized bed hydrodynamics have been the subject of study for many years now.

* Corresponding author. Address: Laboratory of Chemical Reactor Engineering, Eindhoven University of Technology, P.O. Box 513, 5600 MB Eindhoven, The Netherlands. Tel.: +31-40-247-4712; fax: +31-40-244-6653.

E-mail address: j.vanderschaaf@tue.nl (J. van der Schaaf).

0301-9322/02/$ - see front matter
PII: S0301-9322(01)00090-8

In bubbling fluidized beds especially the gas bubble characteristics, i.e. gas bubble size and velocity, are important for fluidized bed performance. On the one hand, gas bubbles provide mixing of the particles, thus enhancing heat and mass transfer; on the other hand, the gaseous reactants in the gas bubbles are barely contacted with catalyst particles, decreasing the reactor efficiency. Knowledge of these gas bubble characteristics is thus needed in order to properly design fluidized bed reactors.

The gas bubble characteristics can be investigated with direct measurement methods which measure the voidage in a fluidized bed, viz. optical, capacitance, and radioactive methods. Optical and capacitance methods provide local information on voidage with the disadvantage that only a small portion of the gas bubble is detected. With radioactive methods more global information can be obtained, but these methods are more expensive and are generally restricted to small-scale fluidized beds.

Instead of determining the gas bubble characteristics directly through voidage measurements, pressure fluctuations caused by the rising gas bubbles can be taken as an indirect measure of bubble size and velocity. Measuring pressure fluctuations is attractive because it is a relatively simple, non-intrusive, and inexpensive technique, applicable to a wide range of experimental conditions. However, in addition to pressure fluctuations originating from rising gas bubbles, other sources generating pressure fluctuations are present in a fluidized bed too, e.g. bed mass oscillation, bubble coalescence, bubble eruption, and gas turbulence.

In this paper the power spectral density (PSD) of time series of pressure fluctuations is used to characterize the gas bubble characteristics in freely bubbling fluidized beds. In literature, the dominant frequency in the PSD of a fluidized bed is commonly reported and associated with a regular fluctuation of the bed height (Roy et al., 1990). A power-law fall-off is generally observed at higher frequencies in the PSD of voidage and pressure time series. This power-law fall-off can be used to characterize fluidized bed hydrodynamics and to validate fluidized bed models (Ding and Tam, 1994; Nowak et al., 1993). Though the PSD is a commonly applied analysis tool in fluidized bed research, confusion still exists about the physical origin of the dominant frequencies and about the observed power-law fall-off. Therefore, in this paper, a method is proposed to decompose the PSD of time series of pressure fluctuations into its different components. Furthermore, these components are identified with the different physical phenomena underlying the time series of pressure fluctuations in gas–solid fluidized beds.

The proposed method is also applied to gas–solid flow in the riser of a circulating fluidized bed. In the riser, generally two different regions can be discerned: (1) a dense region in the bottom part of the riser with a constant particle concentration and irregularly shaped voids of gas, and (2) a dilute region in the upper part of the riser in which clusters of particles are present. The characteristics of the gas voids and the clusters are important for fluidized bed performance and, here too, the PSD of pressure time series can be decomposed into components corresponding to the physical phenomena underlying the pressure time series.

2. Theory

Most definitions given here can be found in any textbook on spectral analysis, e.g. Priestley (1981), Randall (1987), and Newland (1993); the most important definitions will be discussed

briefly here. The PSD, Φ_{xx}, of a pressure time series $p_x(t)$ measured at position x in a fluidized bed is defined as

$$\Phi_{xx}(f) = \frac{1}{T}\langle \mathscr{F}_x(f)\mathscr{F}_x^*(f)\rangle, \tag{1}$$

where $\mathscr{F}_x(f)$ is the one-sided Fourier transform of $p_x(t)$, determined using a fast Fourier transform algorithm, and $\langle\ \rangle$ denotes ensemble averaging. For two time series measured at positions x and y, the cross power spectral density, Φ_{xy}, is defined as

$$\Phi_{xy}(f) = \frac{1}{T}\langle \mathscr{F}_x(f)\mathscr{F}_y^*(f)\rangle. \tag{2}$$

The value of the cross power spectral density will be high for a given frequency, if the Fourier transforms of both time series at that frequency have a constant phase shift: the time series are *coherent* for that frequency. The exact value of the cross power spectral density depends on the power present in the PSDs of both time series. To eliminate this dependency, the absolute value of the cross power spectral density is normalized with the square root of the PSDs of both time series. The square of this value is known as the coherence, γ_{xy}^2, which ranges from 0 to 1

$$\gamma_{xy}^2(f) = \frac{\Phi_{xy}(f)\Phi_{xy}^*(f)}{\Phi_{xx}(f)\Phi_{yy}(f)}. \tag{3}$$

Although a coherence of unity at frequency f indicates that the time series' PSDs are fully correlated at that frequency, the PSD values in both time series may be different. A coherence of zero indicates that the random time series are not coupled: the power may be equally high in both PSDs, but the random signals are uncorrelated.

The coherence between two time series of fluidized bed pressure fluctuations can be used to distinguish the different components in the pressure fluctuations. Bubble coalescence, gas flow fluctuations, bubble eruption, and bed mass oscillation generate a fluctuation in gas velocity causing a pressure wave that travels upwards and downwards in the bed from the point of origin. These pressure waves are measured almost instantaneously throughout the entire bed because of their high propagation velocity. Their amplitudes decrease linearly with distance from the point of origin to the bed surface but do not decrease in the downward direction as was shown experimentally by van der Schaaf et al. (1998). Thus, these pressure waves are *also* measured in the plenum of the fluidized bed and will thus be coherent with the in-bed positions. In addition to the fast-traveling waves, also gas bubbles and turbulence are measured in the fluidized bed. These phenomena only generate a local fluctuation in pressure and not a pressure wave traveling through the fluidized bed. Therefore, these phenomena are *not* measured in the plenum. Consequently, the pressure time series that is measured at some in-bed position, $p_y(t)$, can be described as a function of the pressure time series, $p_x(t)$, that is measured simultaneously in the plenum

$$p_y(t) = a_y(t)p_x(t + \Delta) + b_y(t), \tag{4}$$

where $a_y(t)$ quantifies the attenuation of the coherent fast pressure waves, Δ is the time delay, and $b_y(t)$ is the contribution of gas bubbles or turbulence to the in-bed measured pressure time series. The coherence between the plenum and the measurement position in the bed can be used to indicate whether the phenomena generating fast-traveling waves are dominant, corresponding to a

high coherence, or whether the gas bubbles or turbulence are dominant, corresponding to a low coherence. Of course, the gas distributor plate must not distort the downward-traveling pressure fluctuations: a high pressure drop over the gas distributor plate can damp the pressure fluctuations. If the gas distributor plate does distort the pressure signal, measurements from within the fluidized bed just above the gas distributor plate can be used instead.

The power in the pressure time series at in-bed measurement position y, which is coherent and incoherent with the pressure time series measured in the plenum (x), can be expressed in terms of the coherent-output PSD (COP_{xy}) and incoherent-output PSD (IOP_{xy}), representing the PSDs due to fast pressure fluctuations and due to gas bubbles or turbulence, respectively

$$\mathrm{COP}_{xy}(f) = \gamma_{xy}^2 \Phi_{yy}, \tag{5}$$

$$\mathrm{IOP}_{xy}(f) = (1 - \gamma_{xy}^2)\Phi_{yy}. \tag{6}$$

From the coherent-output and incoherent-output PSDs, the standard deviation of the coherent pressure fluctuations, $\sigma_{xy,\mathrm{c}}$, and the standard deviation of the incoherent pressure fluctuations, $\sigma_{xy,\mathrm{i}}$, can be calculated, according to Parseval's theorem

$$\sigma_{xy,\mathrm{i}}^2 = \int_0^\infty \mathrm{IOP}_{xy}(f)\,\mathrm{d}f, \qquad \sigma_{xy,\mathrm{c}}^2 = \int_0^\infty \mathrm{COP}_{xy}(f)\,\mathrm{d}f. \tag{7}$$

Substituting Eq. (4) into Eqs. (5)–(7) expresses the physical significance of the coherent and incoherent standard deviations

$$\sigma_{xy,\mathrm{i}}^2 = \langle b_y(t)^2 \rangle = B_y^2, \qquad \sigma_{xy,\mathrm{c}}^2 = \langle a_y^2(t) p_x^2(t) \rangle = A_y^2 \sigma_x^2. \tag{8}$$

Thus, the coherent standard deviation gives information on the average pressure fluctuation intensity of fast pressure waves. The average attenuation of these fast pressure waves can be determined from the coefficient A_y. More importantly, the incoherent standard deviation gives information on the amplitude of pressure fluctuations caused by rising gas bubbles, solids clusters, and turbulence. The pressure amplitude due to a rising gas bubble is proportional to the gas bubble diameter and, as will be discussed later, a characteristic measure for the average gas bubble size can be obtained from the incoherent standard deviation. The same arguments hold for solids clusters. Consequently, for the first time, the gas bubble diameter and solids cluster size can be estimated from non-intrusive measurements of pressure time series. This is demonstrated in this paper for the case of a bubbling and a circulating fluidized bed.

3. Experiments

3.1. Bubbling fluidized bed

Time series of pressure fluctuations were recorded in a 0.385 m ID bubbling fluidized bed filled with Geldart-B sand particles ($d_\mathrm{p} = 0.39$ mm, $\rho_\mathrm{s} = 2650$ kg/m^3, $u_\mathrm{mf} = 0.14$ m/s). The settled bed height was 0.30 m (solids inventory = 51.8 kg), and the superficial gas velocity ranged from 0.20 to 0.95 m/s. In each experiment pressure time series were recorded simultaneously along column

height and in the plenum. The in-bed pressure probes were located at 0.04, 0.09, 0.14,0.19, 0.24, and 0.29 m above the gas distributor plate and were mounted flush with the wall.

The pressure fluctuations were measured with Kistler piezo-electric pressure transducers, type 7261. This pressure transducer measures pressure relative to the average pressure by using a high-pass filter with a cut-off frequency of 0.16 Hz. Consequently, the average of the measured pressure time series is zero. The accuracy of this sensor is approximately 2 Pa. The sensors were connected to 0.10 m long copper tubes of 4 mm ID, the total dead volume of sensor and tube was 2500 mm^3. The tubes were equipped with 40 μm mesh wire gauze at the tips, to prevent particles from entering. This set-up has been tested for distortion of pressure fluctuation amplitude and phase (Van Ommen et al., 1999). No significant influence was found at frequencies typical for gas–solid fluidized beds (0–50 Hz). The data was recorded with a SCADAS II data acquisition system from Difa Measurement Systems (LMS, Breda, Netherlands). The time series consisted of 262,144 data points measured with a sample frequency, f_s, of 80 Hz and filtered at 40 Hz using parallel sample and hold with a total acquisition time of 2.4 μs and 16 bit A/D conversion. The PSD and coherence were calculated for each data set of 512 points (NFFT) and were averaged over a total of 512 data sets.

3.2. Circulating fluidized bed

Pressure time series were also recorded in a 4 m high, 0.083 m ID riser of a circulating fluidized bed with Geldart-B sand particles ($d_p = 0.21$ mm, $\rho_s = 2650$ kg/m^3, $u_{mf} = 0.05$ m/s) at a superficial gas velocity of 4.0 m/s and solids mass flows ranging from 49.9 to 101 kg/(m^2 s). The entrained particles were separated from the gas flow by two cyclones and were fed back into the column at a height of 0.12 m. The pressure probes were mounted flush with the wall at heights of 0.06, 0.19, 0.38, 1.87, and 3.12 m and in the plenum. The time series consisted of 720,896 data points sampled at 800 Hz and filtered at 400 Hz. The PSD and coherence were estimated for each data set of 2048 points and were averaged over 352 data sets. Because the total amount of solids in the riser increases with increasing solids mass flow, the average pressure profile along the riser was recorded with differential pressure transducers (Honeywell, 143PC01D and 163PC01D). Contrary to the Kistler sensors, no dynamic information is obtained with these sensors, only the average pressure is obtained at the measurement positions. The pressure profile is given in Fig. 1 for each solids mass flow. The local solids concentration is equal to the derivative of the pressure profile divided by $-\rho_s g$. In the region where the pressure decreases linearly with measurement height, a dense bed with a constant voidage is located.

4. Results and discussion

4.1. Bubbling fluidized bed

For the bubbling fluidized bed typical PSDs are given in Fig. 2 at different measurement heights and at a gas velocity of 0.70 m/s. Typically, the PSDs display a power-law fall-off at high frequencies with a slope of approximately −4. This power-law fall-off was observed for all gas velocities. The PSD decreases in power with increasing measurement height. If the PSDs were

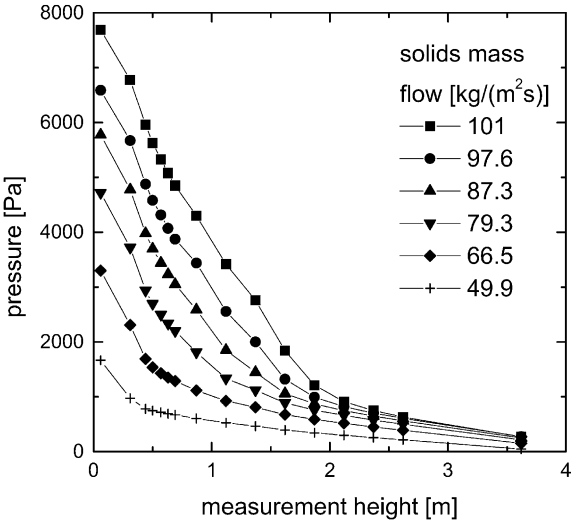

Fig. 1. Pressure profile along 0.083 m ID circulating fluidized bed riser operated at a gas velocity of 4.0 m/s and at various solids mass flows.

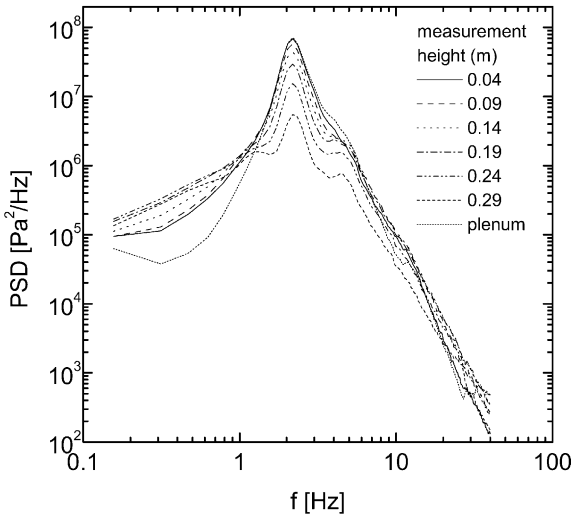

Fig. 2. PSDs at different measurement heights in a bubbling fluidized bed of 0.385 m ID at a gas velocity of 0.70 m/s. At all measurement heights a characteristic power-law fall-off is observed.

caused by pressure fluctuations of gas bubbles only, the opposite would be expected: higher in the bed larger bubbles with higher pressure amplitudes are present. However, in addition to the pressure fluctuations caused by rising gas bubbles, pressure fluctuations originating from other sources, e.g. bubble coalescence, formation, and eruption, are measured with high amplitude. Thus, the direct measurement of gas bubble characteristics from single pressure time series only is impossible for a freely bubbling fluidized bed.

With the time series measured in the plenum, the coherent output PSD, COP_{xy}, was calculated for each measurement height and gas velocity. The COP_{xy} is shown as a function of measurement height for a gas velocity of 0.70 m/s in Fig. 3. Here, a constant power-law fall-off for all measurement heights cannot be observed. The power decreases more rapidly with increasing frequency when compared to the PSD in Fig. 2.

In the COP_{xy} curve, generally a well-defined sharp peak is present for each gas velocity. The corresponding average amplitude of the pressure fluctuations at this peak in the COP_{xy} curve can be calculated by multiplication of the peak value with twice the width of the frequency interval for which the peak value is found, i.e. f_s/NFFT^*2, and taking the square root of this value. In Fig. 4, this amplitude is plotted against measurement height. At all gas velocities the same trends are observed. Near the bed surface the amplitude decreases linearly, which is characteristic for upward-traveling pressure waves (van der Schaaf et al., 1998). The linear dependency on distance-to-bed-surface levels off in the bottom region of the bed. This suggests that the dominant sources of the pressure fluctuations originate from the bottom region of the bed. If the sources were actually located at one fixed position in the bed, a sharp transition from a linear decrease of power to a constant power would be observed (van der Schaaf et al., 1998).

Because in a freely bubbling bed the sources of pressure fluctuations originate from different positions, the transition from a linear decrease of amplitude to a constant amplitude is not sharp but more gradual. This is visually demonstrated in Fig. 5 where the average amplitude resulting from two pressure fluctuations with different origin are plotted. In view of the experimentally determined amplitude decrease with measurement height, it can be concluded that the major part of the coherent pressure fluctuations is generated in the region from zero to 0.19 m above the distributor plate. Consequently, regarding the origin of the coherent pressure waves,

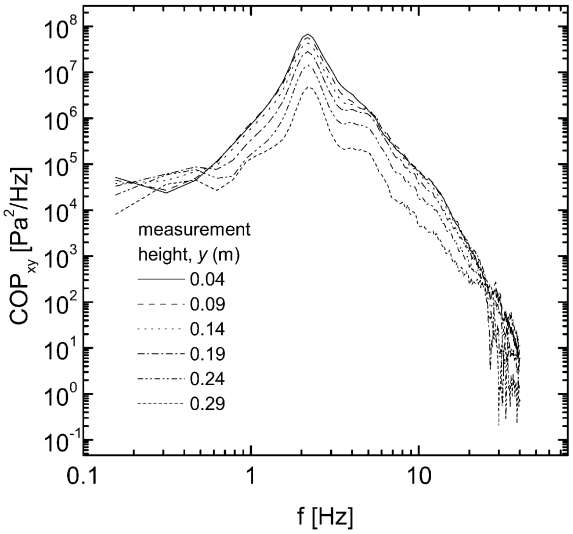

Fig. 3. The coherent-output PSD (COP_{xy}) with x for plenum and y for measurement position, in the bubbling fluidized bed at a gas velocity of 0.70 m/s. The power decreases with increasing measurement height.

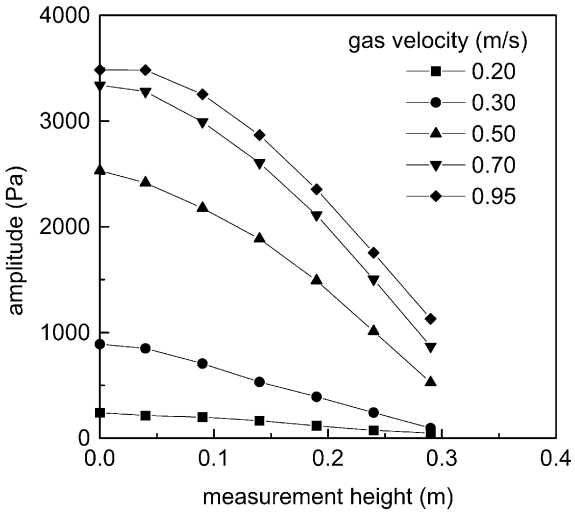

Fig. 4. Average pressure amplitude at COP_{xy} maximum, cf. Fig. 3, versus measurement height. Near the bubbling bed surface, the amplitude decreases linearly. At lower measurement heights, the amplitude levels off.

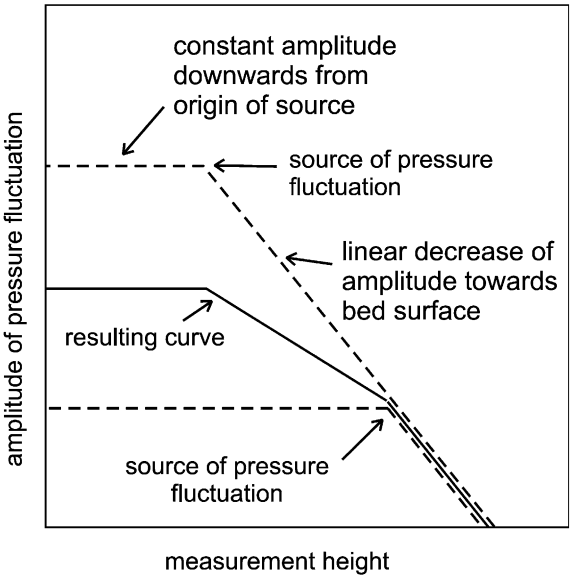

Fig. 5. The gradual transition from linearly decreasing to constant amplitude of fast pressure fluctuations in case of different origins of the sources of the pressure fluctuations (cf. Fig. 4).

the underlying physical phenomenon can only be bubble coalescence and bubble formation, which is consistent with earlier findings (van der Schaaf et al., 1998).

The incoherent output power spectral density, IOP_{xy}, is displayed in Fig. 6 as a function of measurement height for a gas velocity of 0.70 m/s. The lOP_{xy}, dominates the PSD at the higher

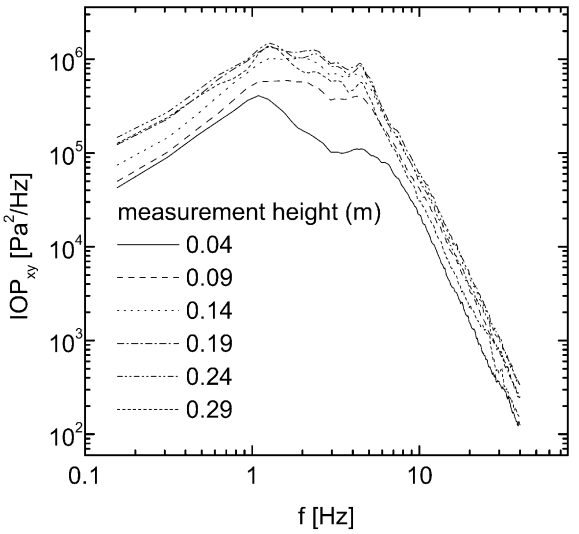

Fig. 6. The incoherent-output PSD (IOP$_{xy}$) for all measurement heights in the bubbling fluidized bed at a gas velocity of 0.70 m/s. The IOP$_{xy}$ increases up to 0.19 m after which the power levels off and decreases near the bed surface. The power-law fall-off is the same for all heights.

frequencies and the characteristic power-law fall-off is clearly coupled to the lOP$_{xy}$, cf. Figs. 2 and 3. Since the IOP$_{xy}$ corresponds to pressure fluctuations caused by gas bubbles and/or turbulence, the power-law fall-off is thus due to either of these phenomena.

Whether turbulence or gas bubbles constitute the IOP$_{xy}$ can be investigated by comparison of the coherence of an in-bed measurement position with the plenum and the coherence of that position with adjacent in-bed measurement positions. Since turbulence is expected to have a very low spatial coherence, it will not increase the coherence between in-bed positions when compared with the coherence between plenum and in-bed positions. Gas bubbles however, are expected to have a much higher spatial coherence and will cause a higher coherence between in-bed measurement positions. For a measurement height of 0.24 m and a gas velocity of 0.70 m/s, the coherence with the plenum and the other measurement heights is shown in Fig. 7. Clearly, the coherence is higher between in-bed measurement positions when compared to the coherence between the in-bed measurement position and the plenum. The coherence increases as the distance between the in-bed probes decreases, a clear indication of the existence of a spatially coherent phenomenon, viz. gas bubbles. Consequently, the IOP$_{xy}$ and the power-law fall-off at high frequencies in the PSD are characteristic for the gas bubble dynamics. The coherence does not reach unity for closely spaced measurement heights because some gas bubbles will have coalesced or accelerated, and will thus have generated an incoherent signal. As the distance between the measurement positions increases, the probability of coalescence increases and the coherence decreases accordingly, cf. Fig. 7.

With the IOP$_{xy}$ now gas bubble dynamics can be investigated as a function of measurement height and gas velocity. Because the IOP$_{xy}$ displays a broad distribution of power over a frequency range up to 10 Hz, the incoherent standard deviation of the pressure time series is calculated from

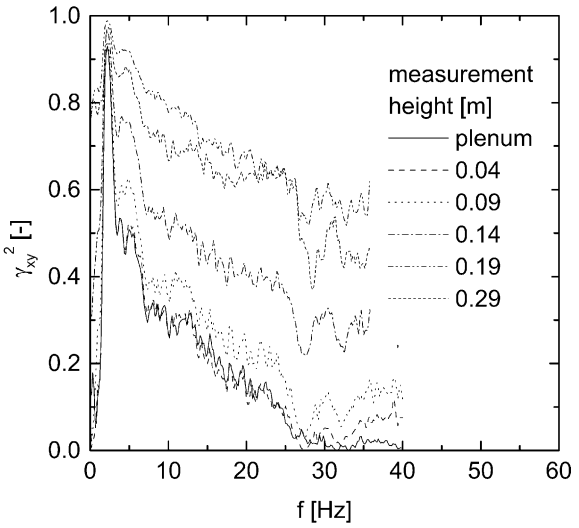

Fig. 7. The coherence (γ_{xy}^2) of the measurement height of 0.24 m with the plenum and with other positions in the bubbling fluidized bed at a gas velocity of 0.70 m/s. The coherence decreases with increasing distance between positions, indicating the presence of a spatially coherent phenomenon.

the IOP_{xy}. The incoherent standard deviation is displayed as a function of measurement height at different gas velocities in Fig. 8. For all gas velocities, this 'gas bubble' standard deviation increases almost linearly up to a measurement height of 0.14 m, implying gas bubble growth. At higher measurement heights, the 'gas bubble' standard deviation levels off and even decreases. In the vicinity of the bed surface the pressure amplitude caused by a rising gas bubble is determined by the particle mass present above the bubble. As the gas bubble rises to the surface this mass decreases and eventually becomes zero as the gas bubble erupts at the bed surface.

The increase of the incoherent standard deviation with measurement height up to 0.19 m in Fig. 8 can be understood with the model for bubble growth by Darton et al. (1977). The Darton model gives the bubble diameter as a function of gas velocity and the height in the bed

$$D_b = 0.54(u - u_{mf})^{0.4} h^{0.8} / g^{0.2}, \tag{9}$$

where h is the height in the bed, u is the superficial gas velocity, and u_{mf} is the minimum fluidization velocity of the particles. If gas bubbles regularly pass the measurement position with frequency f_b, and the resulting pressure fluctuation has a sine wave shape with an amplitude proportional to the gas bubble diameter (Stewart, 1968), this pressure signal caused by gas bubbles, $b_y(t)$, can be represented as

$$b_y(t) = A_b \sin(2\pi f_b t), \quad A_b = \rho_s g(1 - \epsilon_{mf}) D_b. \tag{10}$$

Thus, the standard deviation of the pressure fluctuations caused by the rising gas bubbles, σ_b, is directly proportional to the amplitude of the pressure fluctuations, $\sigma_b = A_b/\sqrt{2}$, in case of a sine wave shape. Though the pressure fluctuations obtained from rising gas bubbles are not sine wave

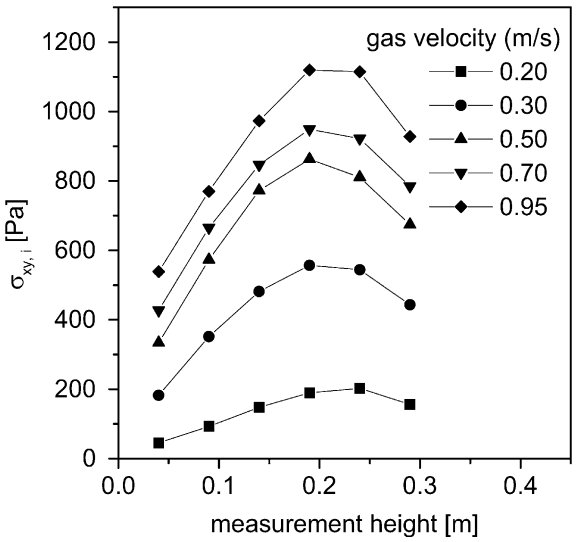

Fig. 8. The standard deviation of the incoherent pressure fluctuations ($\sigma_{xy,\mathrm{i}}$) versus measurement height in the bubbling fluidized bed for different gas velocities. The standard deviation increases up to 0.19 m for all gas velocities, corresponding to gas bubble growth.

shaped but are of a more complex shape, still the standard deviation will be proportional to the amplitude, $\sigma_{\mathrm{b}} \sim A_{\mathrm{b}}$. Hence, from the incoherent standard deviation a characteristic length scale can be derived, which will be proportional to the average bubble diameter

$$\sigma_{xy,\mathrm{i}}/(\rho_{\mathrm{s}} g(1-\epsilon_{\mathrm{mf}})) \sim D_{\mathrm{b}}, \tag{11}$$

where ϵ_{mf} is the bed voidage at minimum fluidization ($\approx$0.45). The relationship between Eqs. (9) and (11) is displayed in Fig. 9 for measurement heights up to 0.19 m. For all gas velocities the characteristic length scale of Eq. (11) corresponds well to the bubble diameter predicted by Darton et al. (1977) according to Eq. (9). At the lowest gas velocity of 0.20 m/s, the bubble size seems to be underestimated while at the higher gas velocities the bubble size seems somewhat overestimated. Thus, from the incoherent output PSD of measured pressure fluctuations a very reasonable estimate of the average bubble diameter can be obtained.

4.2. Circulating fluidized bed

The analysis method discussed so far for bubbling fluidized beds can also be applied to gas–solid flow in the riser of a circulating fluidized bed. The PSD for the circulating fluidized bed operated at a gas velocity of 4.0 m/s and a solids mass flow of 101 kg/(m^2 s) is given for all measurement heights and the plenum in Fig. 10. Because the pressure drop of the distributor plate is much higher than in the case of the bubbling fluidized bed, the amplitude of the pressure fluctuations traveling from within the bed to the plenum is dampened, at some frequencies more

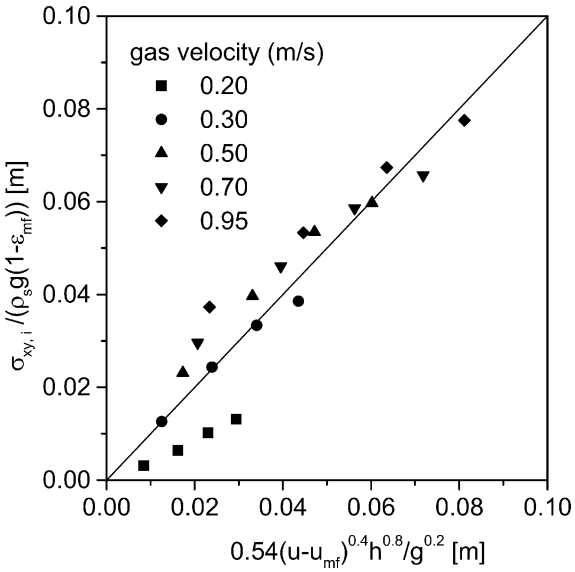

Fig. 9. The characteristic length scale from the incoherent standard deviation (Eq. (11)) versus the bubble diameter predicted by Darton et al. (1977) (Eq. (9)).

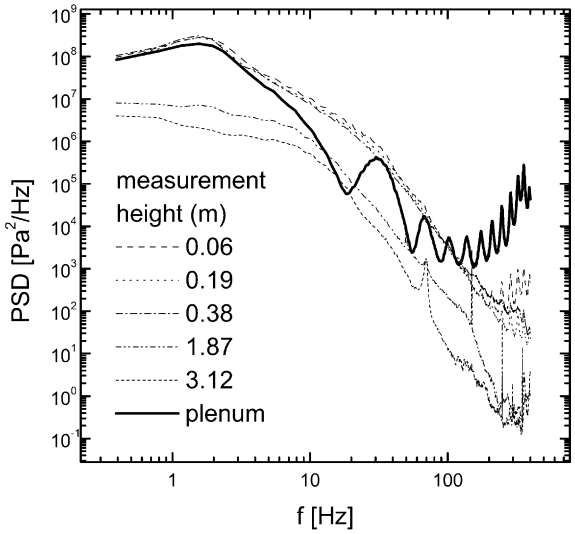

Fig. 10. The PSD at different measurement heights in a 0.083 m ID circulating fluidized bed operated at a gas velocity of 4.0 m/s and a solids mass flow of 101 kg/(m^2 s).

than at others. We will assume here that the attenuation and the corresponding phase distortion is independent of amplitude and does not change in time for each frequency, though it is different for each individual frequency. Also, a strong resonance in the air supply system generates strong pressure fluctuations above 100 Hz, of which the frequencies above 200 Hz are also observed at

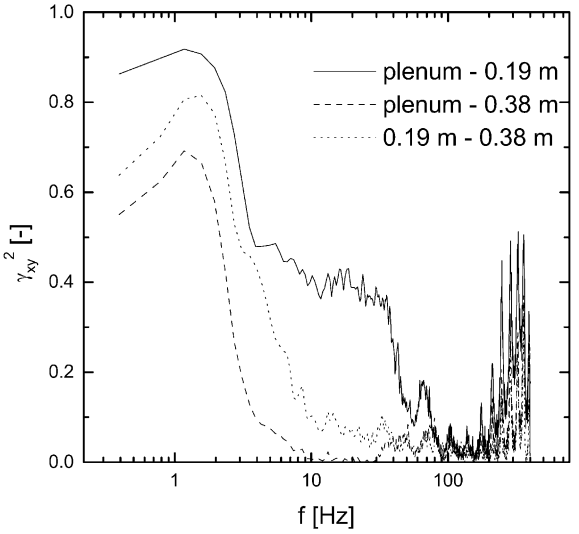

Fig. 11. The coherence (γ_{xy}^2) between the plenum and measurement heights of 0.19 and 0.38 m in the dense region (≈0–1.7 m, cf. Fig. 1) of the circulating fluidized bed.

measurement positions 0.06 and 0.19 m. However, the amplitude of these fluctuations is low compared to the power present in the PSD below 10 Hz, and does not affect the results.

Again, the coherence between in-bed measurement positions can be used to assign a physical phenomenon to the incoherent part of the PSD. In the circulating fluidized bed this is done for the dense region and for the dilute region.

For the dense region, the coherence between the plenum and the in-bed positions at 0.19 and 0.38 m is depicted in Fig. 11. The coherence between the plenum and 0.19 m is high for the peak frequency of approximately 1 Hz and decreases to a value of 0.4 for the frequency range of 4–40 Hz. The coherence between the plenum and 0.38 m is still high around 1 Hz but is approximately zero for the frequency range of 4–40 Hz: consequently, only local phenomena generate power in this frequency range. The coherence between 0.19 and 0.38 m is low but not zero, indicating that still some spatial coherence exists. Therefore, it is likely that rising gas voids are the main source for the incoherent part of the PSD. The spatial coherence of these gas voids is much less when compared to rising gas bubbles in the bubbling fluidized bed due to continuous coalescence and splitting and the erratic movement of the voids.

For the dilute region in the circulating fluidized bed, the coherence between the plenum and the in-bed positions at 1.87 and 3.12 m is shown in Fig. 12. The coherence between the plenum and both measurement heights is approximately equal while the coherence between both in-bed positions is much higher: a strongly spatial-coherent structure is thus present in the dilute region of the circulating fluidized bed corresponding to particle clusters, the only spatial-coherent source of pressure fluctuations in the dilute region. Because small particle clusters generally will not have a high spatial coherence and will most likely change in size and shape when traveling from 1.87 to 3.12 m, the observed high spatial coherence is explained by the presence of mainly large particle clusters or plugs in the dilute region, a commonly encountered phenomenon in circulating fluidized beds with a small riser diameter (Arena et al., 1992).

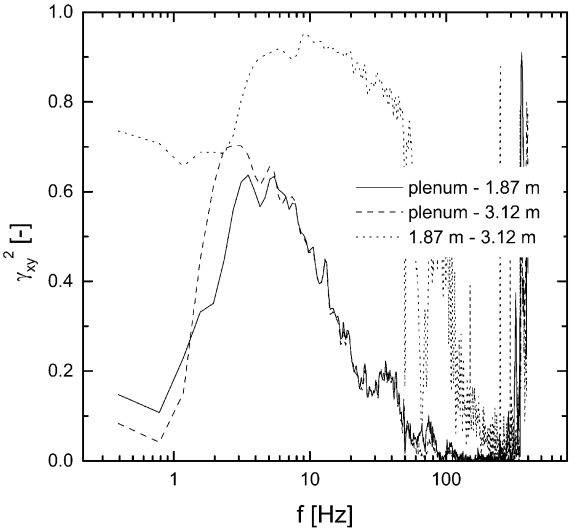

Fig. 12. The coherence (γ_{xy}^2) between the plenum and measurement heights of 1.87 and 3.12 m in the dilute region (>1.7 m, cf. Fig. 1) of the circulating fluidized bed.

The standard deviation of the coherent pressure fluctuations calculated from the COP_{xy} at different solids mass flows is given in Fig. 13. The trends observed for the coherent standard deviation are comparable to the bubbling bed case. The coherent pressure fluctuations originate from the bottom of the dense bed in the riser. Because a solids concentration profile exists along the riser, the amplitude of the coherent fluctuations is determined by the amount of solids above

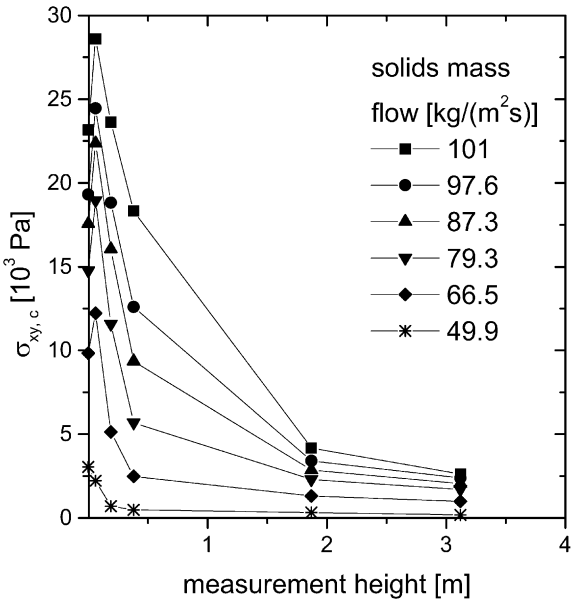

Fig. 13. Coherent standard deviation ($\sigma_{xy,c}$) versus measurement height for different solids mass flows in the 0.083 m ID riser of the circulating fluidized bed. The coherent standard deviation closely follows the pressure profile in Fig. 1.

the measurement position, which is equivalent to the pressure at the measurement position. Comparison of Fig. 13 with the pressure profiles in Fig. 1 shows that the coherent standard deviation indeed has the same dependence on measurement height and solids mass flow. The standard deviation of the pressure fluctuations below the distributor plate is lower than the one above the distributor plate due to the dampening of the pressure waves discussed earlier.

If a solids cluster of volume V_c and with a voidage of ϵ_{mf} passes a measurement position in an upward direction, the pressure increases at this position with

$$\delta p = \frac{\rho_s g(1-\epsilon_{mf})V_c}{\text{riser area}}, \tag{12}$$

until the cluster is separated from the gas flow. Eq. (12) also holds for a gas void in a dense bed, though in that case the pressure would decrease by δp. Similar to the derivation of Eq. (11), the characteristic volume of the solids cluster, V_c, or the gas void, V_v, can thus be estimated from the incoherent standard deviation with

$$\sigma_c/\rho_s g(1-\epsilon_{mf}) \sim V_c/(\text{riser area}), \qquad \sigma_v/\rho_s g(1-\epsilon_{mf}) \sim V_v/(\text{riser area}), \tag{13}$$

with $\sigma_{xy,i} = \sigma_c$ or $\sigma_{xy,i} = \sigma_v$. If the solids clusters and the gas voids are assumed cylindrical with a diameter equal to the riser diameter, thus resembling the typical "plug and slug" structures reported by Arena et al. (1992), a characteristic length scale is given by $\sigma_{xy,i}/\rho_s g(1-\epsilon_{mf})$, which is depicted in Fig. 14. In the dense bed at the bottom of the riser, the characteristic length scale continues to increase, representing the size of the gas void. For the high solids mass flows, the length scale reaches rather high values (~1–1.5 m), corresponding to the size of the slugs of gas rising in the dense bed. These high values agree with results by Arena et al. (1992) who found gas

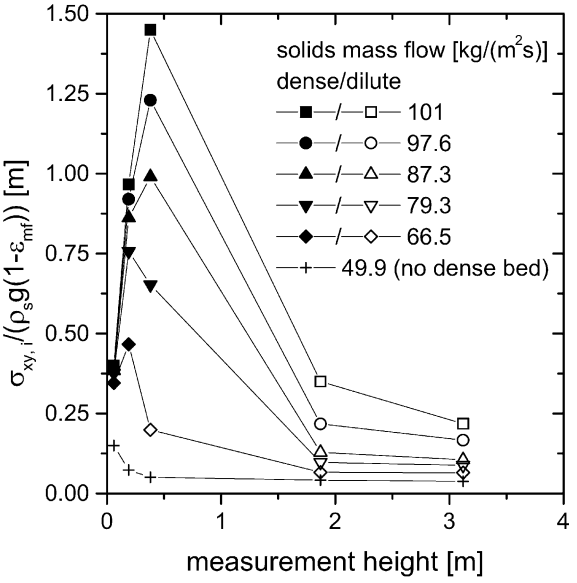

Fig. 14. The incoherent standard deviation ($\sigma_{xy,i}$) divided by $\rho_s g(1-\epsilon_{mf})$ representing the characteristic length scale of either gas voids in the dense bed region (closed symbols) of the riser or solids clusters in the dilute region above the dense bed (open symbols).

slugs of 1 m up to 4 m length in circulating fluidized bed risers of 0.12 and 0.40 m ID. In the dilute region above the dense bed region, smaller sized plugs of solids are present which decrease in size with increasing measurement height.

5. Conclusions

By using the coherence between time series of pressure fluctuations measured simultaneously in a fluidized bed and in its plenum, the PSD of the time series can be split up into the coherent-output and incoherent-output PSDs. In bubbling fluidized beds, the power in the coherent-output PSD is generated by fast pressure fluctuations originating primarily from bubble coalescence and bubble formation. The power in the incoherent-output PSD corresponds to pressure fluctuations generated by passing gas bubbles. The power-law fall-off of approximately power -4 in the PSD is only found in the incoherent-output PSD. Apparently, the power-law fall-off is characteristic for the gas bubble dynamics. With the standard deviation of the incoherent pressure fluctuations calculated from the incoherent-output power spectrum, a characteristic bubble length scale is determined, which agrees well with the bubble diameter predicted by the model proposed by Darton et al. (1977). Thus, with this analysis method, an estimate for the gas bubble size is obtained from measured pressure fluctuations only, which is attractive when direct measurement methods for bubble characteristics are not available. The method can also be used for the characterization of circulating fluidized bed hydrodynamics. The characteristic length scales for gas voids in the dense bed region of the circulating fluidized bed riser can be estimated, as well as the characteristic length scales of solid clusters above the dense bed region.

References

Arena, U., Marzocchella, A., Massimilla, L., Malandrino, A., 1992. Hydrodynamics of circulating fluidized beds with risers of different shape and size. Powder Technol. 70, 237–247.

Darton, R.C., La Nauze, R.D., Davidson, J.F., Harrison, D., 1977. Bubble growth due to coalescence in fluidised beds. Trans. Inst. Chem. Eng. 55, 274–280.

Ding, J., Tam, S., 1994. Asymptotic power spectrum analysis of chaotic behavior in fluidized beds. Int. J. Bifurc. Chaos 4, 327–341.

Newland, D.E., 1993. An Introduction to Random Vibrations and Spectral and Wavelet Analysis, third ed. Longman Scientific/Wiley, New York.

Nowak, W., Matsuda, H., Win, K.K., 1993. Diagnosis of multi-solid fluidized beds by power spectrum analysis of pressure fluctuations. In: Preprints 4th International Conference on Circulating Fluidized Beds, Somerset, PA, USA, pp. 163–168.

Priestley, M.B., 1981. Spectral Analysis and Time Series. Academic Press, London.

Randall, R.B., 1987. Frequency Analysis, third ed. Bruël & Kjær, Denmark.

Roy, R., Davidson, J.F., Tupogonov, V.G., 1990. The velocity of sound in fluidised beds. Chem. Eng. Sci. 45, 3233–3245.

Stewart, P.S.B., 1968. Isolated bubbles in fluidised beds—theory and experiment. Trans. Inst. Chem. Eng. 46, T60–T66.

van der Schaaf, J., Schouten, J.C., van den Bleek, C.M., 1998. Origin, propagation and attenuation of pressure waves in gas–solid fluidized beds. Powder Technol. 95, 220–233.

Van Ommen, J.R., Schouten, J.C., vander Stappen, M.L.M., van den Bleek, C.M., 1999. Response characteristics of probe-transducer systems for pressure measurements in gas–solid fluidized beds: how to prevent pitfalls in dynamic pressure measurements. Powder Technol. 106, 199–218.